Topics in Catalysis Vol. 38, Nos. 1–3, July 2006 (© 2006)
DOI: 10.1007/s11244-006-0076-8

Vanadium oxide surfaces and supported vanadium oxide nanoparticles

S. Guimond[a], M. Abu Haija[a], S. Kaya[a], J. Lu[a], J. Weissenrieder[a], S. Shaikhutdinov[a], H. Kuhlenbeck[a], H.-J. Freund[a,*], J. Döbler[b], and J. Sauer[b,*],

[a]*Department Chemical Physics, Fritz-Haber-Institut der MPG, Faradayweg 4-6, D-14195 Berlin, Germany*
[b]*Institute of Chemistry, Humboldt-Universität zu Berlin, Unter den Linden 6, D-10099 Berlin, Germany*

The information obtained from the characterization of vanadium oxide single crystal surfaces is related to the study of vanadia nanoparticles supported on silica and alumina thin films, model systems for the so-called ''supported monolayer vanadia catalysts''. It is found that these particles have properties similar to V_2O_3 surfaces, where the topmost V ions are involved in vanadyl groups and have a 5+ oxidation state. A vibrational spectroscopy investigation combined with DFT calculations show that the accepted interpretation of vibrational spectra from vanadia catalysts must be revised.

KEY WORDS: vanadium oxide; alumina; silica; scanning tunneling microscopy (STM); photoelectron spectroscopy (PES); DFT calculation; infrared (IR) spectroscopy

1. Introduction

Vanadium oxides are materials of considerable interest in oxidation catalysis [1–3]. Their surface properties, stoichiometric structure and chemical reactivity, however, are widely unexplored, in particular, with respect to systems where surface structure and reactivity could be directly related. Given that for real catalyst systems vibrational spectra are often used to indirectly infer structure on systems [4] that detach themselves from direct surface structure investigations, it is necessary to calibrate those vibrational studies with respect to model systems where morphology and structure can be directly addressed.

In the present paper we will present the characterization of vanadium oxide surfaces and relate this information to supported vanadia nanoparticles, which serve as model systems for so-called ''supported monolayer vanadia catalysts''.

2. Experimental

The experiments have been performed in a number of different ultrahigh vacuum apparatus, which are all located at the Fritz-Haber-Institute in Berlin or at the BESSY II storage ring. They are multipurpose instruments allowing for preparation in chambers separated from the measurement chambers. They have been described in detail in previous publications [5,6].

*To whom correspondence should be addressed.
E-mails: freund@fhi-berlin.mpg.de; sek.qc@chemie.hu-berlin.de

3. DFT calculations

Density functional theory (DFT) is applied for calculating the structures and vibrational frequencies of vanadium oxide surfaces, thin films, nanoclusters and supported vanadium oxide species. The calculations have been described in detail before and use both periodic boundary conditions [7–9] and finite cluster models [10,11].

4. Results and discussion

Figure 1 shows photoelectron spectra of three different vanadium oxides taken with the same photon energy (i.e. He II radiation) and recorded with the same analyzer system. Therefore the changes in the intensity distributions reflects to first order changes in the densities of states in the three systems, i.e. V_2O_5, VO_2, V_2O_3. In all cases particularly stable surfaces have been prepared by either cleavage of a bulk sample ($V_2O_5(001)$), or by epitaxial growth on another oxide ($VO_2(110)$) or metal ($V_2O_3(0001)$) support [6]. The bulk terminated surfaces are shown as schematic representations on the right hand side of the corresponding spectra. The binding energies are referenced to the Fermi level (E_F). The broad structure starting at 3 eV binding energy for V_2O_5 and whose onset shifts to almost 4 eV towards V_2O_3 is due to emission from oxygen and vanadium levels in the oxide band structure formed. The intensity near E_F (grey area) is due to emission from the partially occupied V3d levels. The intensity basically reflects the V3d occupation. Vanadium ions in V_2O_5 are in the highest oxidation state and exhibits no V3d occupation,

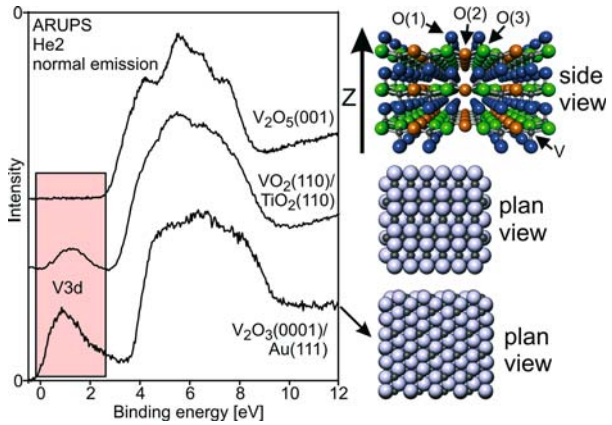

Figure 1. Comparison of valence photoelectron spectra of V_2O_5, VO_2 and V_2O_3.

while upon reduction to VO_2 and further on to V_2O_3 the V3d occupation increases by 2 electrons per vanadium ion. Thus, the photoelectron spectra nicely reflect the expected electronic structure of the bulk material. However, it is not easily possible to deduce surface information from those spectra. In the following we will address the structure and transformations at the surface of vanadium oxides, using V_2O_3(0001) as an example.

Figure 2 shows the stable V_2O_3(0001) surface prepared under reducing conditions. As the corresponding surfaces of isostructural Cr_2O_3(0001), Fe_2O_3(0001) and Al_2O_3(0001), this surface is terminated by a layer of vanadium ions representing half of the buckled vanadium ion layer along the (0001) direction in the bulk [12]. Judged by the strong relaxation on the surface layers with respect to the bulk observed for Cr_2O_3(0001) [13], Fe_2O_3(0001) [14] and Al_2O_3(0001) [15] it is reasonable to assume that the V_2O_3(0001) surface is strongly relaxed also, i.e., the vanadium ions relax strongly inward sitting almost in plane with the underlying oxygen layer. The schematic shown in figure 1 (right side) corresponds to this state of the V_2O_3(0001) surface. Upon exposure of the surface to oxygen from the gas phase, eventually, a layer of adsorbed oxygen atoms forms that are bound directly to the underlying vanadium atoms via an oxygen–metal double bond effectively forming a surface vanadyl (V=O) species. The vanadyl species, which is a well-known moiety from vanadium chemistry, is characterized by a typical V–O vibrational frequency in the range of 1000 cm^{-1} [4]. Note, that the vanadyl moiety is only present at the surface, and its presence would not have been anticipated on the basis of the bulk structure; it is V_2O_5 that contains vanadyl bonds within its bulk structure. This has lead researchers in the past to assume that the presence of vanadyl species is intimately connected with the presence of V_2O_5 in some form. The present study shows that this is not necessarily the case. DFT calculations have also confirmed the large tendency of metal terminated (0001) surfaces of V_2O_3 crystals [16] and thin films [7,8] to cover with oxygen atoms forming vanadyl surface groups.

We can follow the formation of the vanadyl species on the V_2O_3(0001) surface by dosing oxygen at low temperature onto the reduced surface. Figure 3 shows the vibrational spectra recorded after an exposure at 90 K. Two features are found, one of which develops at higher temperature to the well-known vanadyl species. The second feature around 950 cm^{-1}, which has previously been observed for Cr_2O_3(0001) where isotopic labeling has been used to avoid confusion [17], can be identified as η^2-peroxo species [18]. Once room temperature is reached all peroxo species have been converted into vanadyl oxygen species. We know from the corresponding studies for Cr_2O_3(0001) that the additional oxygen desorbs above 300 K [17]. In the latter case there is hardly any mixing with the lattice oxygen of the Cr_2O_3(0001) observed.

The frequency of 950 cm^{-1} of the η^2-peroxo species (formally O_2^{2-}) is consistent with an O–O bond that is significantly longer than in gas phase O_2 and also longer than in superoxo species (formally O_2^-). Table 1

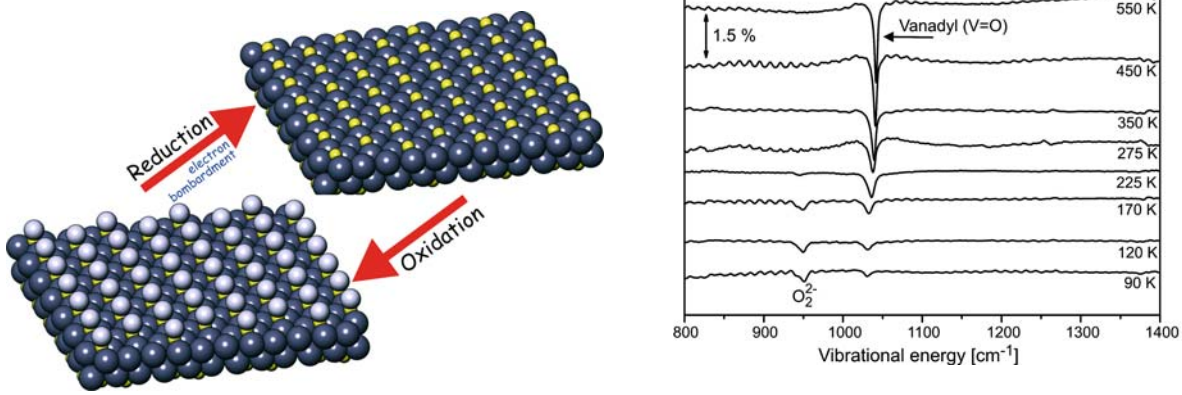

Figure 2. Schematic representation of V_2O_3(0001) surface under reducing and oxidizing conditions.

Figure 3. Fourier Transform IR absorption spectra of a reduced V_2O_3(0001) surface after dosing 15 L molecular oxygen at 90 K and heating to the indicated temperature.

Table 1
Bond distances, R_{OO} (Å), and vibrational frequencies ν_{OO} (cm^{-1}) of different oxygen species on the $V_2O_3(0001)$ surface and on model compounds

Type		Calcd[a] R_{OO}	Calcd[a] ν_{OO}	Obsd ν_{OO}
Molecule	$^3O_2$ gas phase	1.21	1524	1556
η^2-Superoxo	$V_2O_6^+$	1.29	1175	1160
η^1-Superoxo	$V_2O_7^-$	1.31	1138	1112
Superoxo	$^2O_2^-$ gas phase	1.35	1102	1090[e]
η^2-Peroxo	$O_2VSi_7O_{12}H_7$ [b]	1.43[b]	984[b]	
	$O_2/V_2O_3(0001)$[c]	1.44[c]	960[c]	951
	V_4O_{11}	1.41	957	
	$VO(O_2)(C_2O_4)_2^{3-}$	(1.43)[d]		904[d]
Peroxo	H_2O_2	1.47	886	878
Vanadyl (O=V)	$OVSi_7O_{12}H_7$ [b]	1.58[b]	1033[b]	
	V_4O_{10}	1.57	1039	
	$O/V_2O_3(0001)$ [c]	1.61 [c]	1029[c]	1030–1040

[a] B3LYP functional/TZVP basis set, scale factor 0.9429 [19].
[b] Ref [24].
[c] Ref [18], PW91 functional, scale factor 0.95812 derived as ν_{OO}(Obsd)/ν_{OO}(Calcd) for PBE on $V_4O_{11}^-$ [20].
[d] Distance obsd., see Ref. [25] for references to the original work.
[e] Estimated from experimental data for LiO_2 and NaO_2 for O_2^- well separated from counterion, Ref. [26].

shows computational and experimental results on which this assignment is based. DFT calculations (B3LYP functional) have been made for the gas phase species O_2, $V_2O_6^+$ (η^2-superoxo), $V_2O_7^-$ (η^1-superoxo) and O_2^-. The increasing distance in this series is explained by an increasing population of antibonding orbitals when passing from O_2 to O_2^- and O_2^{2-}. Accordingly and in agreement with experiments, the frequencies decrease in this sequence. This is an example for the importance of joint experimental (IR laser spectroscopy) and computational (DFT) studies on gas phase vanadium oxide ions [19,20] for the assignment of vibrational spectra to species on vanadium oxide surfaces. The Table shows frequency ranges of 1160–1090 cm^{-1} for superoxo and 980–880 cm^{-1} for peroxo species, very close to frequency ranges reported for the corresponding surface species [21]. We have made calculations for a periodic model of O_2 on $V_2O_3(0001)$ [18] and for a molecular model of V_2O_3 covered with three vanadyl groups and with one O_2 group, V_4O_{11} (figure 4). The predicted O–O frequencies, 960 and 957 cm^{-1}, respectively, are very close to the observed 951 cm^{-1} and leave no doubt about the assignment to an η^2-peroxo species. We have also made calculations for an η^2-peroxo group on an isolated site of vanadium oxide supported on silica (figure 10 below, model **1a**). Also for this situation the O–O stretching frequency (984 cm^{-1}) is in the expected range. For comparison, the Table shows also the vanadyl frequencies obtained for the same models, which are all three in the 1029–1039 cm^{-1} range.

The O_2 vibration cannot be excited with infrared radiation in the gas phase, however if the molecule binds to the surface, the symmetry is broken, and a spectrum can be recorded. Due to the limited thickness of the oxide film the metal substrate underneath will dominate the response to the exciting IR radiation. Thus metal surface selection rules apply, which implies contradiction with the orientation of the η^2-peroxo species almost parallel to the surface, but in fact is not as a closer analysis shows. The DFT calculation for the V_4O_{11} model system yield a dipole change for the O–O stretch normal mode, n_{OO}, that is oriented perpendicularly to the O–O bond axis (see figure 4). When O_2 binds on a metal site, there is charge transfer from the metal to the O_2 unit, resulting in a $V^{\delta+}-O_2^{\delta-}$ dipole perpendicular to the surface. The magnitude of this dipole depends on the O–O distance. For larger distances, typical of peroxo species it is larger (formally $V^{2+}-O_2^{2-}$) and for smaller distances typical of superoxo species it is smaller (formally $V^{+}-O_2^{-}$). The same happens when the O–O normal mode is excited, the charge separation between V and O_2 changes with the O–O distance and a dipole change perpendicular to the O–O bond is created.

Once the vanadyl oxygen is formed the vanadium ions in the surface change their formal oxidation state,

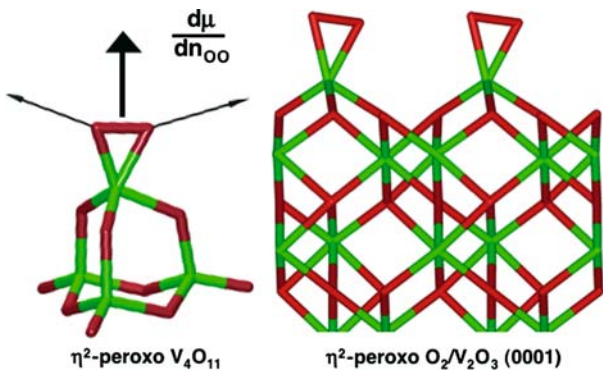

Figure 4. Peroxo species on $V^{3+}(d^2)$ sites: V_4O_{11} and $O_2/V_2O_3(0001)$.

i.e. going from 3+ (on the reduced, metal-terminated surface) to 5+. Dupuis et al. [6] have demonstrated that this may be experimentally corroborated. Figure 5 shows four photoelectron spectra in the range of V2p and O1s (above E_B: 529 eV) ionizations. We concentrate on the discussion of the $V2p_{3/2}$ ionization at lowest binding energy. The spectra have been taken at either normal electron emission ($\Theta = 0°$, sensitive to surface and deeper layers) or at a grazing excidence ($\Theta = 70°$, sensitive predominantly to the surface). Both, the reduced (V-terminated) as well as the oxidized (vanadyl-terminated) surfaces are compared. The vanadium terminated surface shows a $V2p_{3/2}$ state exhibiting a chemical shift compatible with an oxidation state of V^{3+} as in V_2O_3 (taken in a surface sensitive mode, $\Theta = 70°$). This shift is considerably different from the one observed for V_2O_5 where vanadium is in formal oxidation state +5. When we look at the vanadyl terminated surface with surface sensitivity we see a clear broadening of the $V2p_{3/2}$ line. The fitting indicates that there is a component located at the high binding energy side with chemical shift indicative of V^{5+}. This component is attenuated when the spectrum is recorded at normal excidence, indicating that the vanadium ions in higher oxidation state are located in the surface. This is fully compatible with the idea of vanadyl groups on the surface, where the vanadyl vanadium ions are in oxidation state 5+ as opposed to the vanadium ions in the bulk of the material. However, we note that the vanadyl groups belong to four fold coordinated vanadium ions, dissimilar from the situation encountered in V_2O_5, where V is 5-fold coordinated. Further support comes from DFT calculations on the oxidized (vanadyl terminated) V_2O_3 surface [8,16] which show a V2p core level shift of about 1.6 eV [8] to higher binding energies for the V^{5+} ions in the surface layer that are part of the vanadyl groups relative to the V^{3+} ions in the layers underneath.

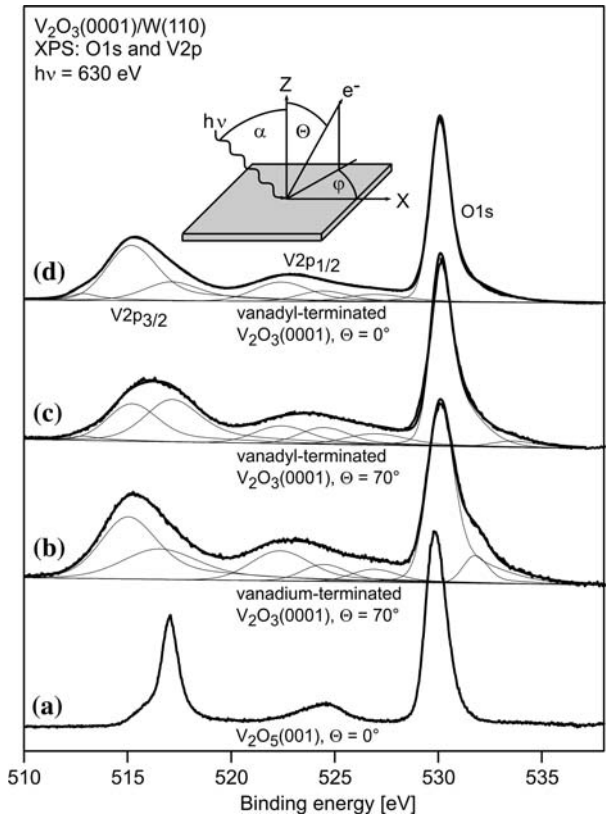

Figure 5. Photoelectron spectra of $V_2O_3(0001)$ and $V_2O_5(001)$ taken at different electron emission angles, Θ.

Figure 6, panel (a) shows an STM image of the vanadyl terminated surface. This represents a 1×1 structure with dimensions of the unit cell compatible with a vanadyl group at the position of all of the vanadium ions in the reduced system. In order to remove the vanadyl groups the system has to be electronically excited which we achieve by electron irradiation. Note, that this is different from the situation found for $Cr_2O_3(0001)$ where chromyl group could be removed thermally [17]. In panel (b) a partially reduced surface is imaged, and on panel (c) an STM image of a surface that has been reduced further is shown. The unit cell of panel (c) is identical to the one in panel (a), and therefore indicative of the presence of the same order at the surface, as anticipated for the reduced surface. As we follow the reduction of the surface via STM images, XP spectra have been recorded, however, with a laboratory source explaining the lower resolution. The spectra are shown in figure 5 and they indicate that the position of the V2p doublet shifts to lower binding energies upon reduction and the O1s intensity is reduced at the same time. Summarizing, the STM data fully support the conclusions based on the IR-spectroscopic information.

Having understood the surface chemistry of solid vanadium sesquioxide, we now turn to deposited vanadia nanoparticles in an attempt to model the situation found in so-called monolayer oxide catalyst. Figure 7 shows STM images of deposited vanadia nanoparticles. Here is the first surprise: in contrast to expectations, the deposited vanadia does not spread to wet the surface! Even at higher coverages, and considering different supports such as silica and alumina, this is not the case, as shown in figure 8. The size of the particles can be estimated on the basis of the panel on the right hand side of figure 7. Here a vanadia nanoparticle is imaged on the atomically resolved silica substrate. Since we know the atomic dimensions of the substrate and we know approximately the effect of tip convolution, we can estimate the size of the particles rather precisely as 10–12 Å. This typically leaves room for vanadia aggregates such as V_2O_5 or V_4O_{10} clusters. This stoichiometry is also consistent with estimates based on the amount of deposited vanadium from quartz-balance measurements and the number of structures seen in the STM. At this point we note that a so-called monolayer catalyst consists of nanoparticles with rather small stoichiometric

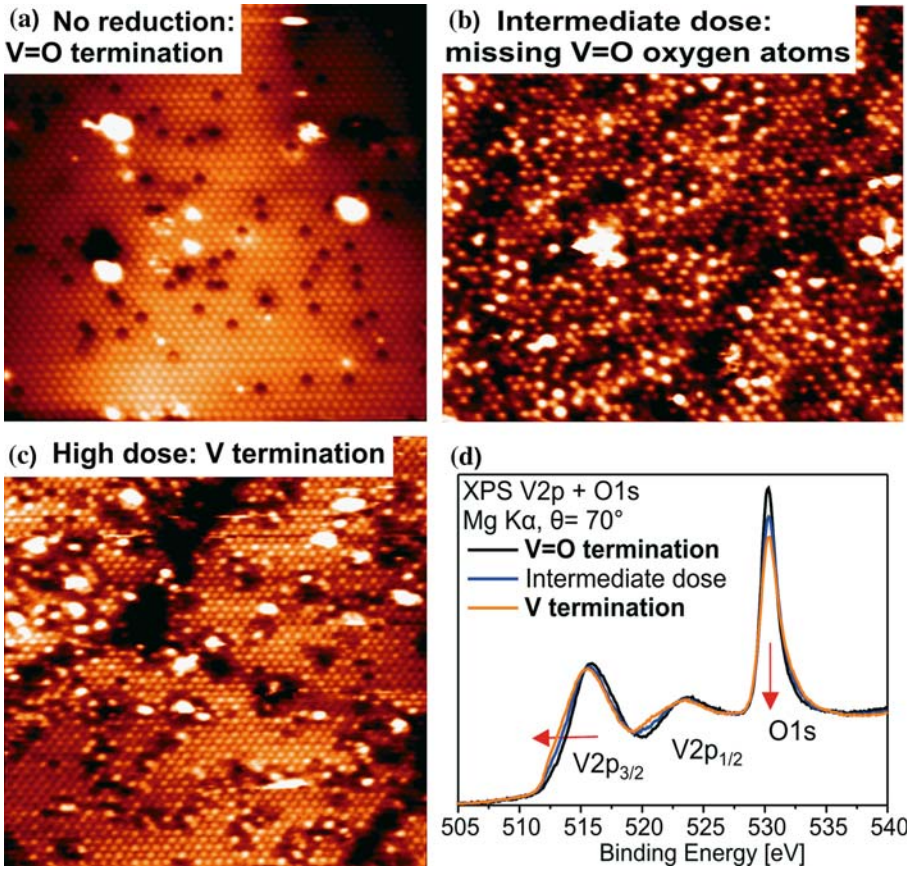

Figure 6. (a–c): STM images (20×20 nm, $U = 2$ V, $I = 0.2$ nA) of vanadyl-terminated (a), weakly reduced (b), and strongly reduced (c) $V_2O_3(001)$ surfaces. Panel (d) shows corresponding XPS spectra.

units and the habit of the nanoparticles is independent of the substrate they are deposited on.

In studies of powder supported vanadia catalysts, Raman Spectroscopy is often employed to unravel structural characteristics of the material [4]. Here, the vibrations between 700 and 1100 cm^{-1} are used as fingerprints to identify units related to so-called monomeric and/or polymeric species. The position of the vanadyl vibration around 1000–1050 cm^{-1} is often used as an indicator and a differentiator for such species. Also, a characteristic band occurring around 950 cm^{-1} is taken to represent the presence of polymeric V_xO_y species. The presence of this latter band for VO_x/alumina and its absence in the case of VO_x/silica is such an

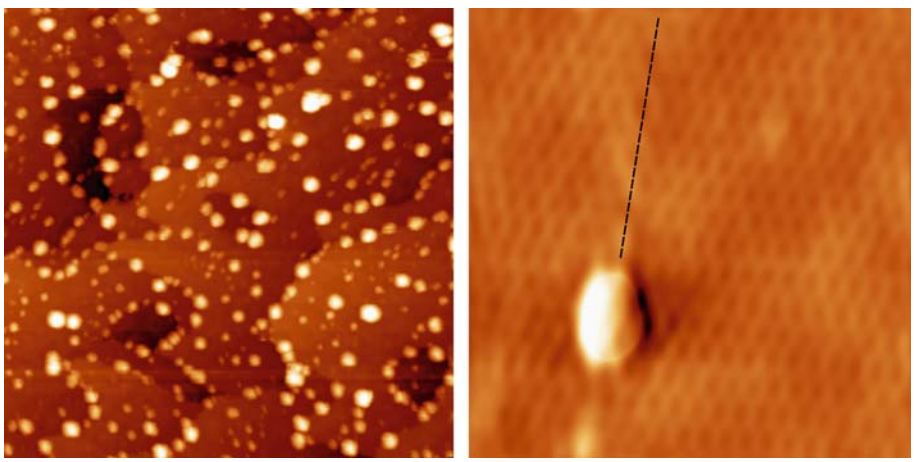

Figure 7. STM images of vanadia nanoparticles deposited on a model silica surface (SiO_2/Mo(112)). Left image: 100×100 nm, $U = 3$ V, $I = 0.2$ nA. Right image: 10×10 nm, $U = 1.5$ V, $I = 0.2$ nA.

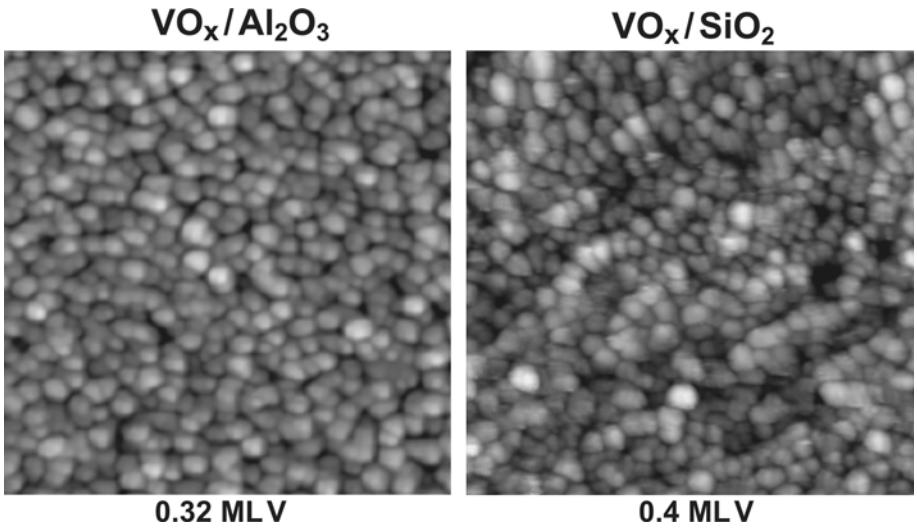

Figure 8. STM images (50×50 nm) of vanadia nanoparticles grown on a model alumina ($Al_{10}O_{13}$/NiAl(110)) and a model silica (Si_4O_{10}/Mo(112)) thin film. Left image: $U = 2.2$ V, $I = 0.07$ nA. Right image: $U = 3.3$ V, $I = 0.12$ nA.

example. This is a good test case for model studies, where vibrational spectroscopy, in this case Fourier transform infrared spectroscopy, may be applied. Figure 9 shows the vibrational spectra of VO_x/alumina and VO_x/silica model catalyst. The data were taken on samples which were prepared in the same way as those, whose STM images have been shown in figures 7 and 8.

The spectra shown have been recorded for the clean supports (at the top) and then for samples where the coverage of VO_x particles has been systematically increased. The spectra for VO_x/alumina are considerably different from those recorded for VO_x/silica. In particular, the characteristic band at 940 cm^{-1} shows up for VO_x/alumina but not for VO_x/silica. The finding correlates very well with the above mentioned powder studies. However, note once more, that the morphology of the two model systems as imaged with STM is almost indistinguishable. If, however, the absence of the 940 cm^{-1} band for VO_x/silica was primarily due to the absence of polymetric species, the similarity of the samples would be hard to explain.

To assist the assignment of the spectra DFT calculations have been performed on finite models for VO_x on both supports [11], and on periodic models for VO_x/alumina [7,9]. Figure 10 shows some of the models adopted and figure 11 shows the frequency ranges in which characteristic vibrational modes are found. For monomeric species on SiO_2 (figure 10, model **1**) three different bands can be distinguished: vanadyl stretch (1040–1050 cm^{-1}), in-phase stretch of the three V–O(–Si) bonds (around 1010 cm^{-1}) and the two corresponding out-of-phase V–O(–Si) stretch modes (870–900 cm^{-1}). The IR intensities of all three bands are of the same order of magnitude [11]. For the dimeric vanadium oxide species (model **2**) the wave number ranges of these three types of vibrations expand. This is due to couplings, e.g. between the two vanadyls but also due to an increased heterogeneity of local surface

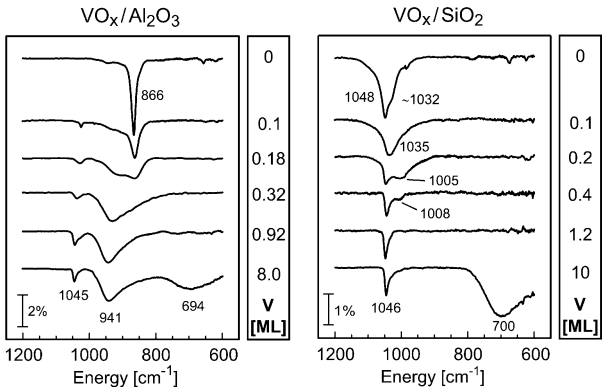

Figure 9. FT-IRAS spectra of clean (top) $Al_{10}O_{13}$/NiAl(110) (a) and Si_4O_{10}/Mo(112) (b) surfaces and after growing vanadia nanoparticles at different coverages given in monolayers (ML).

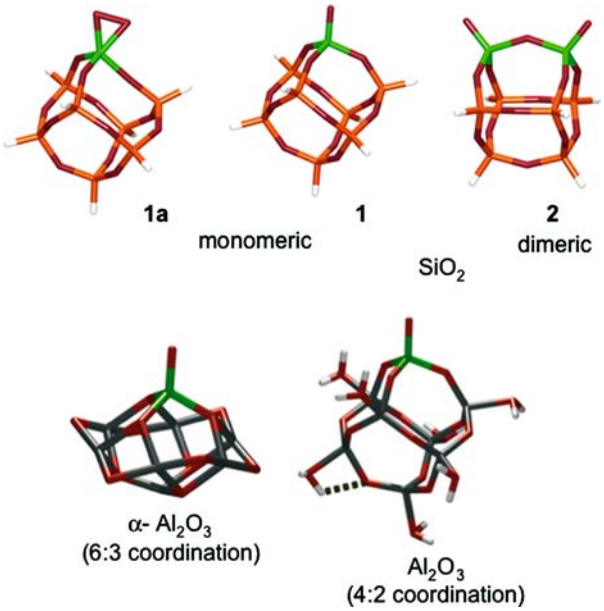

Figure 10. Models for silica- and alumina-supported vanadium oxide.

structures as represented by additional models shown in figure 2 of Ref. [11]. The frequencies of the V–O–V modes fall into the range 735–825 cm^{-1}, much lower than the 950 cm^{-1} assumed in the literature. Despite their high intensity, the V–O–V modes will be hard to detect because this region of the spectrum is usually dominated by framework vibrations of the silica support.

For the alumina support, the vanadyl bands are in a similar range as for the silica support, but the V–O(–Al) interphase modes show large frequency changes. For the α-Al_2O_3 support the in-phase coupling and the two out-of-phase couplings are only little separated at 796 and 771 cm^{-1} (calculations for model **3**) [11]. Calculations for an ultrathin V_2O_5 film on α-Al_2O_3 support these results. The vibrations of the three-fold coordinated V–O–(Al)Al interface atoms are in the 805–745 cm^{-1} range [7]. For V_2O_5 clusters on α-Al_2O_3 the V–O(–Al) modes of the interphase O atoms cover a broad range of wavenumbers that extends from 775 cm^{-1} up to 925 cm^{-1} and covers also a narrow range around 800 cm^{-1}, in which V–O–V vibrations are found. The reason for the higher wavenumbers is that the V–O–Al interphase atoms are two-fold coordinated whereas the V–O–(Al)Al interphase atoms in the thin V_2O_5 film on α-Al_2O_3 are three-fold coordinated. A further shift of the V–O(–Al) interface bands is found for an Al_2O_3 support in which Al is tetrahedrally coordinated and O is two-fold coordinated (figure 10, model **4**). The four most intense bands fall in the region between 955 and 925 cm^{-1}. It is known that the alumina support, used to prepare the VO_x/Al_2O_3 model catalysts, contains tetrahedrally coordinated Al [22,23] and, therefore, the observed prominent band at 940 cm^{-1} (figure 9) is assigned to an V–O(–Al) interface vibration.

Hence, the DFT calculations on various models lead to a complete and consistent assignment of the observed spectra for the VO_x/silica and VO_x/alumina samples as discussed in more detail in Ref. [11]. While the band due to an interfacial V–O–Al-vibration is found around 940 cm^{-1}, the corresponding V–O–Si vibrations overlap strongly with the vanadyl vibration and can lead to a more complex behavior of the vibrational spectra in the range around 1000–1050 cm^{-1}.

This is also born out by the spectral series in figure 9. The silica phonons are in the same range as the vanadyl band and lead to a complex spectral function

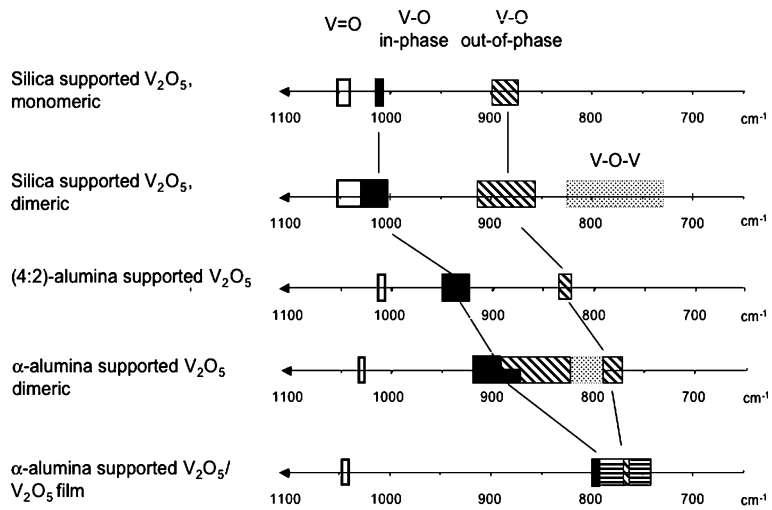

Figure 11. Wavenumber ranges for V=O (vanadyl) and V–O(-M) interphase modes for different vanadium oxide species and different supporting oxides. Data from Ref. [11], for α-alumina supported dimeric V_2O_5 from Ref. [9] and for α-alumina supported V_2O_5 film from Ref. [7]. For the latter, in phase and out-of-phase V–O(-M) modes cannot be distinguished and the range of V–O(-2Al) vibrations is marked by horizontal stripes.

as the coverage is increased. At highest coverage one basically only sees the vanadyl vibration. For VO_x/alumina the situation is different. The position of the vanadyl band is considerably different from the highest energy alumina phonon band. When these energetically separated vibrations are coupled to form the interfacial vibration, a new band at an intermediate ($\sim$940 cm^{-1}) position shows up. The behavior as a function of coverage is then rather simple. At highest coverage both the vanadyl as well as the interface band survive. The band showing up for the highest coverages below 800 cm^{-1} is due to V–O–V phonons well known for the V_2O_3 bulk. That these particles contain vanadium in formal oxidation state +3 is also recovered through electron spectroscopic studies. The latter finding is not a surprise since we know from the above studies on the V_2O_3(0001) surface that vanadyl groups are the surface terminators under oxygen-rich conditions.

We note here in passing only the fact that further corroborating evidence for the revised assignment of the 940 cm^{-1} band as an interfacial mode can also be brought about through vibrational measurements using CO as a probe molecule. We have looked at the influence of CO on the vibrational modes at the two, i.e. VO_x/alumina and VO_x/silica systems and varied the coverage of VO_x in such a way that in one case the interface is accessible for CO while in a high coverage case it is inaccessible. This has been discussed in detail elsewhere [11].

The final issue in our comparison between V_2O_3 single crystal surfaces and VO_x/support is the reduction of the fully vanadyl covered nanoparticles surface. Figure 12 shows vibrational spectra of VO_x/silica after dosing the surface with CO in saturation coverage (bottom), and after reducing the vanadia nanoparticles partly using an electron beam. Spectra show the CO stretching regime. In the bottom trace a single CO stretching vibration is found that is characteristic of CO molecules interacting with vanadyl groups as observed previously [11]. The trace above shows CO stretching vibration spectra recorded after dosing a partially reduced system. A second CO vibration shows up at lower frequency as a shoulder. This CO species are associated with molecules bound to vanadium ions that have lost their vanadyl oxygen but are still surrounded by other vanadyl groups. The two spectra shown in addition represent situations where the surface of the partially reduced system has been heated to 150 K and 200 K respectively. It is evident that the CO species bound to the defects in the vanadyl covered particles are more strongly bound as compared to those CO molecules interacting with the vanadyl groups only, as the relation intensity of the band at lower energy decreases in intensity less rapidly than the one at higher stretching frequency.

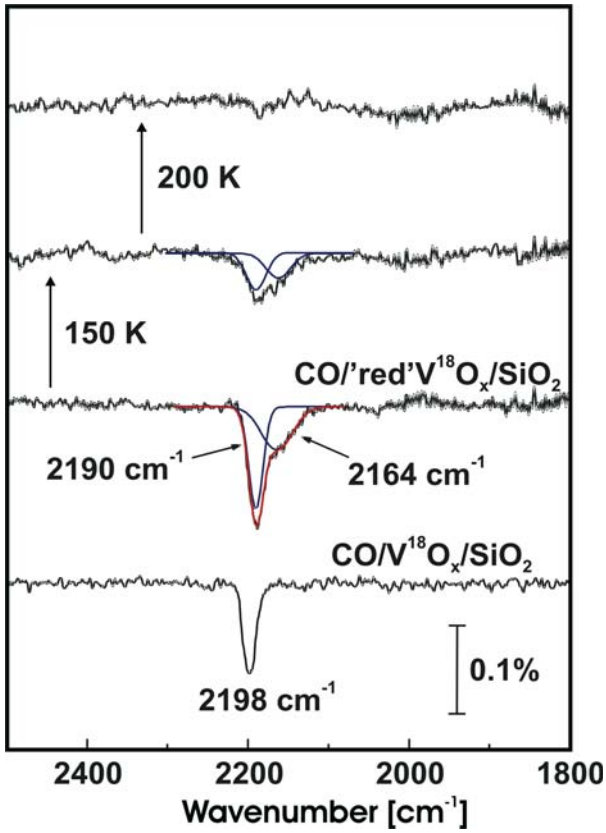

Figure 12. FT-IRAS spectra in the range of CO stretching frequencies for VO_x/SiO_2/Mo(112) exposed to CO. Non reduced system at the bottom in comparison with a reduced system at different temperatures.

In summary, the situation encountered for VO_x/support systems appears to be very similar to the situation on oxide single crystal surfaces.

5. Synopsis

We have compared vanadium oxide single crystal surfaces with the situation on VO_x/supported systems. Unexpectedly, a vanadium sesquioxide surface exposes vanadyl units that have typically only been associated with vanadia (V_2O_5) crystals and surfaces. The vanadium ions involved in the vanadyl groups in the surface of V_2O_3 have an oxidation state similar to vanadium ions in the bulk or at the surface of V_2O_5. Deposited VO_x nanoparticles have been prepared on alumina and silica supports. Their properties resemble the situation found at the V_2O_3 surface. A vibrational study combined with DFT calculations reveals that the previous assignment generally accepted for powder catalyst samples needs to be revised.

Acknowledgments

We are grateful to funding through Sonderforschungsbereich 546 and through the ATHENA project

founded by the EPSRC. The ''Fonds der Chemischen Industrie'' is also gratefully acknowledged.

References

[1] G.C. Bond and S.F. Tapir, Appl. Catal. 71 (1991) 1.
[2] G. Deo and I.E. Wachs, J. Catal. 146 (1994) 323.
[3] B.M. Weckhuysen and D.E. Keller, Catal. Today 78 (2003) 25.
[4] I.E. Wachs, Catal. Today 100 (2005) 79.
[5] N. Magg, J.B. Giorgi, T. Schroeder, M. Bäumer and H.J. Freund, J. Phys. Chem. B 106 (2002) 8756.
[6] A.C. Dupuis, M. Abu Haija, B. Richter, H. Kuhlenbeck and H.J. Freund, Surf. Sci. 539 (2003) 99.
[7] V. Brázdová, M.V. Ganduglia-Pirovano and J. Sauer, Phys. Rev. B 69 (2004) 165420.
[8] T.K. Todorova, M.V. Ganduglia-Pirovano and J. Sauer, J. Phys. Chem. B 109 (2005) 23523.
[9] V. Brázdová, M.V. Ganduglia-Pirovano and J. Sauer, J. Phys. Chem. B 109 (2005) 23532.
[10] J. Sauer and J Döbler, Dalton Trans. 19 (2004) 3116.
[11] N. Magg, B. Immaraporn, J.B. Giorgi, T. Schroeder, M. Bäumer, J. Döbler, Z. Wu, E. Kondratenko, M. Cherian, M. Baerns, P.C. Stair, J. Sauer and H.J. Freund, J. Catal. 226 (2004) 88.
[12] H. Kuhlenbeck and H.-J. Freund, The Chemical Physics of Solid Surfaces, Vol. 8 (Elsevier, Amsterdam, 1997), p. 340.
[13] BibUnstructured > F. Rohr, M. Bäumer, H.-J. Freund, J.A. Mejias, V. Staemmler, S. Müller, L. Hammer and K. Heinz, Surf. Sci. 372 (1997) L291, Erratum: F. Rohr, M. Bäumer, H.-J. Freund, J. A. Mejias, V. Staemmler, S. Müller, L. Hammer and K. Heinz, Surf. Sci. 389 (1997) 391.
[14] X.G. Wang, W. Weiss, S.K. Shaikhutdinov, M. Ritter, M. Petersen, F. Wagner, R. Schlögl and M. Scheffler, Phys. Rev. Lett. 81 (1998) 1038.
[15] S. Guénard, G. Renaud, A. Barbier and M. Gautier-Soyer, Surf. Rev. Lett. 5 (1998) 321.
[16] G. Kresse, S. Surnev, J. Schoiswohl and F.P. Netzer, Surf. Sci. 555 (2004) 118.
[17] B. Dillmann, F. Rohr, O. Seiferth, G. Klivenyi, M. Bender, K. Homann, I.N. Yakovkin, D. Ehrlich, M. Bäumer, H. Kuhlenbeck and H.J. Freund, Faraday Discuss. 105 (1996) 295.
[18] M. Abu Haija, S. Guimond, Y. Romanyshyn, A. Uhl, H. Kuhlenbeck, T.K. Todorova, M.V. Ganduglia-Pirovano, J. Döbler, J. Sauer and H.-J. Freund, Surf. Sci., 600 (2006) 1497.
[19] K. Asmis, G. Meijer, M. Brümmer, C. Kaposta, G. Santambrogio, L. Wöste, J. Döbler, M. Sierka and J. Sauer, J. Chem. Phys. 120 (2004) 6461.
[20] G. Santambrogio, M. Brümmer, L. Wöste, J. Sauer, G. Meijer and K. Asmis, J. Chem. Phys. (2006), in preparation.
[21] N. Sheppard, Vibrational Spectroscopy of Adsorbates, Springer Series in Chemical Physics, Vol. 15, ed. R.F. Willis (Springer Verlag, Berlin, 1980), p. 165.
[22] R.M. Jaeger, H. Kuhlenbeck, H.J. Freund, M. Wuttig, W. Hoffmann, R. Franchy and H Ibach, Surf. Sci. 259 (1991) 235.
[23] G. Kresse, M. Schmid, E. Napetschnig, M. Shishkin, L. Köhler and P. Varga, Science 308 (2005) 1440.
[24] M. Pritzsche, J. Döbler and J. Sauer (2006), in preparation.
[25] M.S. Reynolds and A Butler, Inorg. Chem. 35 (1996) 2378.
[26] C.J. Cramer, W.B. Tolman, K.H. Theopold and A.L Rheingold, Proc. Natl. Acad. Sci. USA 100 (2003) 3635.